

Improving on the ENCODE ChIP-seq normalization pipeline

Joshua Kim

July 22, 2019

Contents

1	Summary	3
2	Background	3
2.1	DNA, chromatin, and histone modifications	3
2.2	ChIP-seq, ATAC-seq, and more	3
2.3	Mappability	4
3	The Old Pipeline	5
3.1	Umap	5
3.2	align2rawsignal	5
4	The New Pipeline	6
4.1	GenMap	6
4.2	WiggleTools	7
5	Methods	7
5.1	Fragment length estimation	7
5.2	Normalization	8
6	Results	9
6.1	Fragment length estimation	9
6.2	Normalization	9
7	Conclusion	9

1 Summary

This report summarizes the three months I spent at EMBL-EBI in Hinxton, UK, where the primary focus of my work was designing a more efficient implementation of the ENCODE ChIP-seq signal normalization pipeline, known as align2rawsignal [3]. In short, align2rawsignal is a tool written by Anshul Kundaje used to normalize data generated from ChIP-seq based on a variety of criteria, including mappability of the genome, sequencing depth, and replicates. Further, the signal track generated differentiates between regions in the sequence which have no read coverage (denoted by a 0 signal value), and regions which have no signal due because they lie in unmappable areas in the genome (denoted by a *NaN* signal value). It additionally requires mappability tracks generated from a tool called Umap [5] which generates binary mappabilities for a given read length and reference genome. I was able to create a more efficient pipeline, replacing Umap with GenMap [7] and re-implementing align2rawsignal with WiggleTools [9]. In order to better understand the motivation behind this pipeline, I will first briefly explain the biological context, and then give an in depth analysis of the pre-existing pipeline before I show my results.

2 Background

2.1 DNA, chromatin, and histone modifications

DNA is normally organized into beads, known as chromatin, around histone proteins in the nucleus. When in this form, regions of the DNA can become more or less transcriptionally available through processes known as histone modifications. Acetylation and methylation (addition of acetyl and methyl groups resp.) are the most common forms of modifications, and the combination of where the histone is modified and which group is added determines whether the DNA in that chromatin will be more or less active. In addition to histones, there are other proteins which can bind to the DNA and affect gene transcription. One large family of these are known as transcription factors. Often, knowing where a transcription factor binds is an important insight in gene regulation. This can be accomplished in a few ways, but the most common is known as ChIP-seq, which combines chromatin immunoprecipitation with high throughput sequencing. However, it is not always enough to know where a specific protein binds. One may wish to probe more generally at the DNA structure, looking for all accessible regions of the genome. This can be accomplished by techniques such as ATAC-seq and DNase-seq, which use different isolation methods to separate and sequence the open regions of DNA.

2.2 ChIP-seq, ATAC-seq, and more

ChIP-seq [4] is a widely used epigenetic technique to identify regions of interest for a given protein. Primarily used with transcription factors, it can be split into two subprocesses: chromatin immunoprecipitation followed by high throughput sequencing. Chromatin immunoprecipitation is further divided into four steps. First, the DNA and the protein of interest are crosslinked reversibly, via UV light or formaldehyde. Then, the DNA is fragmented into lengths of 200-400 base pairs using either lysates or sonication. Third, the fragments which contain

crosslinked DNA-protein pairs are precipitated out using antibodies to the protein of interest. Finally, the crosslinking is undone and the proteins are digested, while the DNA continues to be purified and sequenced [2]. Once purified, the DNA is then sequenced. The key information with the sequencing step is that the entire fragment is often not sequenced. From a 300 base pair fragment, it is possible, and common, that only 75-100 base pairs from either end will be sequenced. Thus, instead of seeing reads aligning to where the fragment lies in the genome, you will see reads aligning to the start and end of the fragment, with the center of the fragment lacking coverage.

ATAC-seq and DNase-seq are two other common techniques. They are similar to one another in that they probe the entire genome looking for open regions, or regions potentially accessible by proteins. However, ATAC-seq is much more relevant as it requires significantly less time and significantly fewer cells [1]. The difference between these techniques and ChIP-seq is that these show all available locations in the genome, whereas ChIP-seq will show all locations which a specific protein has bound to.

Despite the different use cases for the aforementioned techniques, the resulting data is strikingly similar. They all submit fragments of length 200 or more to be sequenced, resulting in two peaks around the actual fragments when looking at the coverage tracks. Furthermore, the core goal of all of these is the same, to identify regions of interest on the genome by looking at differences in sequencing depth. Thus, for the sake of this report I will just refer to ChIP-seq, but keep in mind that what I say is applicable to more than just ChIP-seq.

2.3 Mappability

One final important concept is the mappability of a genome. Mappability is defined as a measure of how often a specific sequence with length k occurs in the given genome. If the sequence is unique, it is given a mappability of 1, and this value approaches 0 the more frequently the sequence occurs in the genome. Thus, for a given k and genome, one can iterate through the entire genome base by base, and determine the mappability value of the k -mer at each position. From there, one could obtain a binary mappability track by only keeping positions with values of 1, or completely unique positions, and setting all other values less than 1 to 0. Knowing the mappability of a genome can be useful for e.g. preprocessing a fasta file to select only mappable reads.

In this application, the mappability will be used in two ways. The first way will be in the fragment length calculations, where the mappability is used to filter the coverage values to regions that are completely mappable. This improves the accuracy of the fragment length calculation primarily by reducing noise and bias. Ramachandran, et. al showed that differences in mappability can introduce an artificial bias into the fragment length calculation, and by masking the reads for mappability, this bias can be corrected for [8]. The second usage of the mappability is at the normalization step, where the mappability is used to normalize the signal coverage values. If a one region is a highly mappable region, and another region is not, we would expect there to be more reads in the more mappable region. Thus, this is normalized for, so that a highly mappable region does not display a peak where it should not be.

3 The Old Pipeline

Here I will discuss the methods of the previous pipeline, along with any motivation for switching to another pipeline.

3.1 Umap

Umap is a tool developed originally by Anshul Kundaje. The original script was written in MATLAB, but is no longer publicly available. Mehran Karimzadeh then reimplemented Umap using Python in 2016, adding some new features such as calculating the mappability of the bisulfite-converted genome [5]. Umap in its essence is comprised of 3 steps. For a given k value, it will

1. generate all possible k -mers,
2. map each of the k -mers to the genome,
3. and mark all uniquely aligned positions.

The step that is problematic is step 2, where the authors use Bowtie [6] to align each k -mer to the genome. While Bowtie is certainly an industry standard, it is better optimized for actually aligning reads to a reference sequence, not just aligning k -mers to calculate mappability. Thus, the runtime for Umap ends up being approximately 200 CPU hours on a single core, or 30 minutes on 400 cores.

Additionally, Umap has soft requirement that it can only run on Sun Grid Engine (SGE) machines. SGE is a cluster software similar to SLURM or LSF. However, there is no guarantee that every machine uses SGE, and to convert Umap to SLURM or LSF compatible software is tedious and has not yet been publicly done.

3.2 align2rawsignal

Align2rawsignal is another tool developed by Anshul Kundaje, specifically for analysis of ENCODE data [3]. It is also developed in MATLAB, and requires the MATLAB runtime library to execute. As an input, it requires one or more BAM files, along with the fragment length(s) (L_i) for each file. It then proceeds as follows:

1. The read starts are shifted in the 3' direction by $\frac{L_i}{2}$ and then coverage is computed per strand.
2. A weighted sum of read counts is calculated using a Tukey kernel of width w , centered at each position x . This weighted sum $F(x)$ represents the approximate number of sequenced fragments overlapping any position x .
3. The fragment counts from both strands are added together.
4. Steps 1. through 3. are then repeated for the binary mappability track with the same read length, to generate the local cumulative mappability ($M(x)$). $M(x)$ indicates the number of positions around x which can potentially contribute read counts based on mappability.

5. An expected fragment count track is then calculated using the following formula:

$$E(x) = \frac{M(x) * R}{G} \quad (1)$$

where R is the total number of mapped reads in the input file, and G is the total mappable genome size across both strands.

6. The normalized signal $S(x)$ is computed using the formula

$$S(x) = F(x)/E(x) \quad (2)$$

7. Signal values at unmappable regions and at positions where $E(x) \leq \frac{\max_x E(x)}{4}$ are set to *NaN*, so that positions with a value of 0 represent mappable positions where no reads mapped, and positions with no values are completely unmappable positions.

The end result is a normalized signal track $S(x)$, where at each base position x the signal has been normalized by number of reads and mappability. While nothing is inherently wrong with the tool, it is not as efficient as it could be, as it reimplements several things which already have efficient implementations, e.g., reading and writing to standard file formats.

4 The New Pipeline

In the new pipeline, Umap has been replaced by GenMap, and align2rawsignal has been re-written using Python3 and WiggleTools. This introduces several benefits, which are detailed below.

4.1 GenMap

GenMap is a tool written in C++ using the SeqAn library [7]. The principle ideas of GenMap are the same as with Umap: to calculate the mappability for a given length k at each position in the genome. However, GenMap is more efficient than Umap by several orders of magnitude. This is primarily due to a few intelligent choices made in GenMap:

1. The first choice was to use an EPR dictionary, which is an implementation of a bidirectional FM index. This is an alternative to the index used in the Bowtie aligner, which is a unidirectional FM index based on the Burrows Wheeler Transform. The benefit of the bidirectional index is that it supports forward *and* reverse lookups in constant time. Using this, GenMap can take advantage of similar k -mers which share a large portion of their content, and only the beginning and end portions are different.
2. The next choice was the use of optimum search schemes. Optimum search schemes take advantage of a bidirectional FM index to split a text into parts. They dictate which parts of the search string should be searched in what order to minimize the number of errors allowed in the first pieces of each search, thereby limiting the number of edges in the search tree.

3. Finally, mappability values for redundant k -mers are recycled. That is, while computing the mappability of a k -mer, all occurrences of that k -mer in the text will have its mappability value filled in. Then, when that position is encountered later on, it can already be skipped.

By utilizing these improvements, GenMap is able to achieve a runtime of 2.5 minutes on 16 cores, as opposed to 30 minutes on 400 cores with Umap. Additionally, it does not depend on any specific clustering software

4.2 WiggleTools

WiggleTools is another tool written in C++. There are many different functions included within WiggleTools which are used to manipulate and calculate statistics on coverage data. Its main benefit is that it streams in data from input files and then immediately performs online calculations and streams its output, requiring very little memory overhead. For comparison, align2rawsignal loads chunks of the input files into memory, splitting the file by default into 20 chunks. Additionally, WiggleTools doesn't require the MATLAB runtime library, and just requires a default GNU compiler. One other advantage WiggleTools provides is its ability to use standard filetypes as input and output formats. It relies on the HTSLib and libBigWig libraries, which are standard libraries used for input and output of sequencing data. This is crucial because indexed binary files, such as BigWig and BAM files, provide significantly quicker access to the data stored in them.

5 Methods

5.1 Fragment length estimation

The fragment lengths were estimated using pearson correlation values as a measurement:

```

1 def pearson_masc(args, shift):
2     pos_file = "{}pos.bw".format(args.input[:-3])
3     neg_file = "{}neg.bw".format(args.input[:-3])
4     command = "wiggletools pearson strict trimFill trim %s shiftPos
      %d %s unit %s trimFill trim %s shiftPos %d %s shiftPos %d unit
      %s" % (args.map, shift, args.map, pos_file, args.map, shift,
      args.map, shift, neg_file)
5     if args.naive: command = "wiggletools pearson strict %s
      shiftPos %d %s" % (pos_file, shift, neg_file)
6     pearson = float(subprocess.check_output(shlex.split(command)))
7     return pearson, shift

```

The key part of the code is line 4, where `wiggletools pearson` is called. In this line, the pearson correlation values are calculated between the positive and negative strands, where only values in *dual strand mappable* regions are used for the calculation. *Dual strand mappability* is defined as regions where a read mapping to position x on the positive strand, and position $x + \text{shift}$ on the negative strand, are both mappable. This is in contrast to the call on line 7, where a naive pearson correlation is calculated without any regard for mappability. The technique of filtering to only dual mappable regions is adapted from MaSC [8], and does well to reduce artefacts introduced by noise

and random data. However, I found that this was not enough, and resulted in the very first points, corresponding to the read length of the sample, being artificially inflated.

Thus, I introduced one final correction technique, where I ignore any max value if it occurs at the very first shift value, and then I smooth the entire curve using a moving average filter:

```

1     while (maxPearson == pearson_vals[0, 0] and pearson_vals.
      size - (2*args.smooth + 1) > 2):
2         pearson_vals = np.delete(pearson_vals, 0, 0)
3         maxPearson = np.nanmax(pearson_vals[:, 0])
4         if (pearson_vals.size - (2*args.smooth + 1) == 2): sys.exit
      ("Error: Fragment length likely invalid. Continuously downward
      correlation trend.\n")
5         pearson_vals[:, 0] = runningMean(pearson_vals[:, 0], args.
      smooth)
6         maxPearson = np.nanmax(pearson_vals[args.smooth:-args.
      smooth, 0])
7         maxShift = pearson_vals[np.where(pearson_vals[args.smooth:-
      args.smooth, 0] == maxPearson)[0][0], 1] + readlen

```

This is a reasonable assumption to make, as there are two possible scenarios:

1. The max value is always the smallest shift value. This means the trend is a constant negative slope, and there is likely some sort of error in the read data.
2. The max value will eventually jump to another value which is not the left-most shift value. This is much more likely to be the true shift value.

With this, I had a method to calculate the fragment lengths of any input file. I also managed to parallelize it, distributing the pearson correlation calculations among a variable number of input processors.

5.2 Normalization

The normalization method used was a fairly accurate reimplementaion of the original tool by Kundaje [3], so the details won't be elaborated on here. However, I will highlight two small differences.

The first is that Kundaje's tool used read start counts in their signal. In my implementation, I used read coverage counts. Thus, in the normalization calculation, I had to multiply the total mapped read count by the read length, as such:

$$E(x) = \frac{M(x) * R * RL}{G} \quad (3)$$

The only difference to equation 1 is the addition of the RL variable, which represents the read length.

The second difference is that the normalization by Kundaje uses a Tukey kernel to perform an aggregate sum, where the central window length is equal to the fragment length with a weight of 1, and then it tapers on both ends with the weights following a cosine curve. The entire Tukey kernel window is of length 300. In our normalization, we simplify this further and just use a simple windowed sum of length 300.

6 Results

6.1 Fragment length estimation

Figure 1 shows three separate samples to show some preliminary results. Each one was run first with naive Pearson calculations, then with mappability masking, and finally with mappability masking *and* removing the first max values.

As you can see, the peak shifts significantly from the first row compared with rows 2 and 3. This is due to the bias introduced by mappability differences. According to Ramachandran, et. al, using the mappability as a mask was enough to completely eliminate the preference for the read length. However, I found that there was still a strong tendency to overweight the shift values close to the read length. In figure 1, on row 2, the first sample predicted the correct fragment length. However, the following two samples both predicted a length of 76, which corresponds to the read length. Thus, by filtering out those max values occurring in the very beginning, and smoothing the data, we can get much more accurate values, shown in row 3.

6.2 Normalization

The normalization results are difficult to display, as they are very large signal track files. The alternative assessment used was to generate various statistics on the sample files pre- and post-normalization, including area under the curve (AUC), covariance, mean value, and max value.

One interesting note is that although my implementation was very similar to the implementation described in Michael Hoffman’s paper [3], the end results looked a bit different to one another. This can be attributed to a few possibilities.

One possibility is that the differences mentioned in section 5.2 account for more variability in the normalization than anticipated. However, the read length factor in equation 3 should cancel itself out within the data, since the data is read coverage and not read start counts.

Another possibility is that there is an error in align2rawsignal. Looking at figure 2, you see a comparison between track data normalized by align2rawsignal, and track data normalized by my implementation. In the supplementary file of [3], they explain that the final step of the normalization is to discard signal track values which lie in regions of low mappability, or in completely unmappable regions. However, the figure clearly displays a region of low/non-mappability where align2rawsignal fails to remove the signal. This could be why the AUC is so much higher in align2rawsignal.

7 Conclusion

References

- [1] Jason D Buenrostro, Paul G Giresi, Lisa C Zaba, Howard Y Chang, and William J Greenleaf. Transposition of native chromatin for fast and sen-

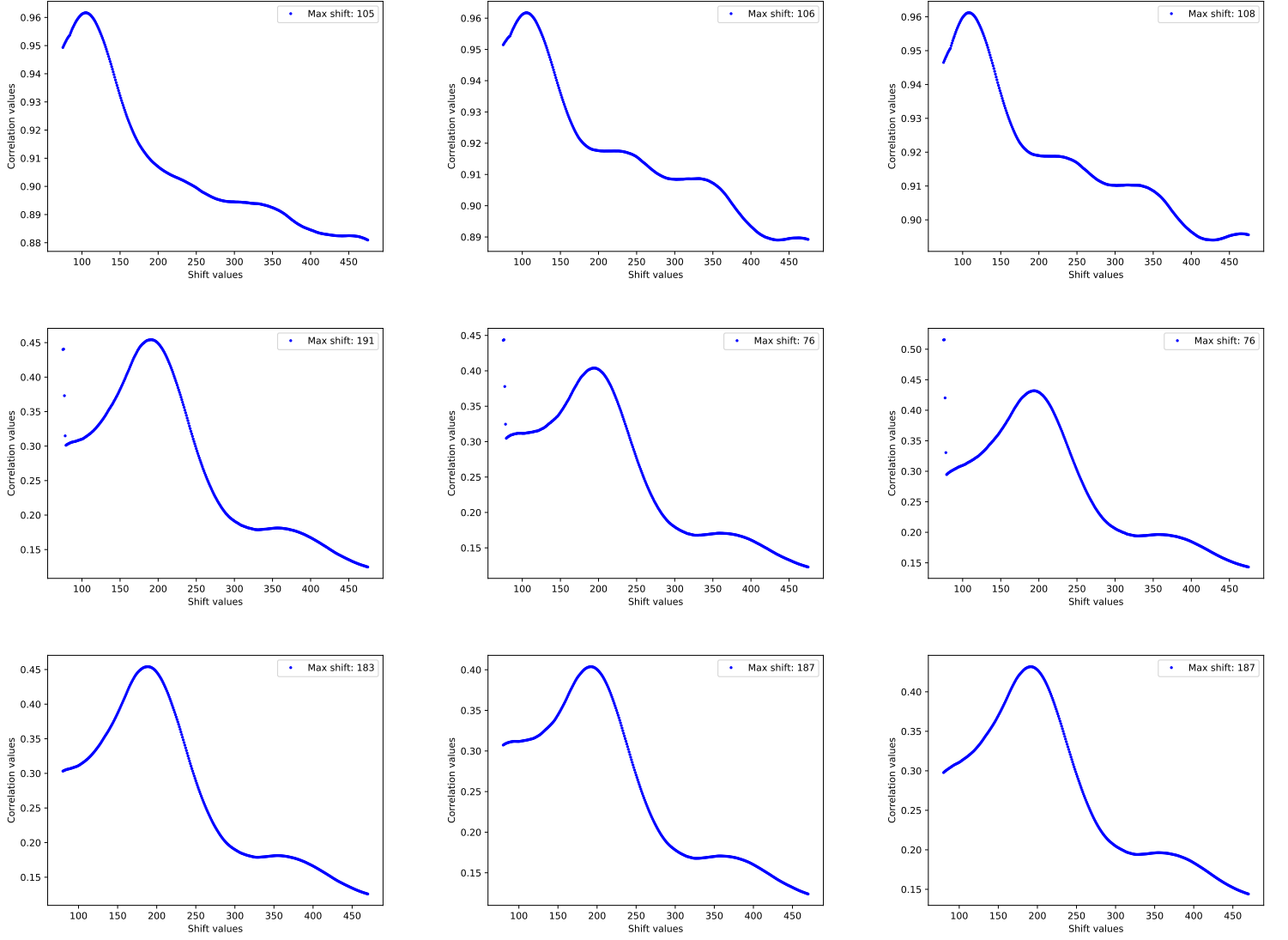


Figure 1: Three samples processed naively (Row 1), using mappability to mask unmappable values (Row 2), and then using mappability and filtering the left-most max values (Row 3). The max shift values are: (Row 1) 105, 106, 108, (Row 2) 191, 76, 76, (Row 3): 183, 187, 187

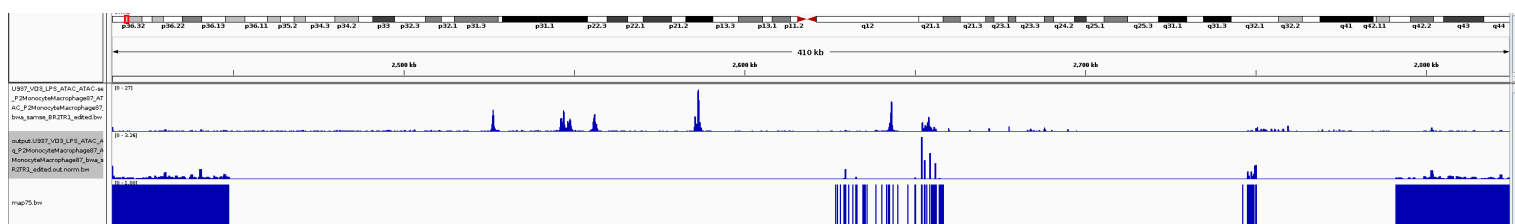


Figure 2: A comparison between Kundaje’s align2rawsignal (track 1) and my reimplement (track 2), with the mappability in this region displayed in track 3. Note align2rawsignal shows non-zero values in unmappable regions, despite claiming to discard signal in these regions.

- sitive epigenomic profiling of open chromatin, DNA-binding proteins and nucleosome position. *Nature Methods*, 10(12):1213–1218, December 2013.
- [2] Philippe Collas. The Current State of Chromatin Immunoprecipitation. *Molecular Biotechnology*, 45(1):87–100, May 2010.
 - [3] Michael M. Hoffman, Jason Ernst, Steven P. Wilder, Anshul Kundaje, Robert S. Harris, Max Libbrecht, Belinda Giardine, Paul M. Ellenbogen, Jeffrey A. Bilmes, Ewan Birney, Ross C. Hardison, Ian Dunham, Manolis Kellis, and William Stafford Noble. Integrative annotation of chromatin elements from ENCODE data. *Nucleic Acids Research*, 41(2):827–841, January 2013.
 - [4] David S. Johnson, Ali Mortazavi, Richard M. Myers, and Barbara Wold. Genome-Wide Mapping of in Vivo Protein-DNA Interactions. *Science*, 316(5830):1497–1502, June 2007.
 - [5] Mehran Karimzadeh, Carl Ernst, Anshul Kundaje, and Michael M. Hoffman. Umap and Bimap: quantifying genome and methylome mappability. *Nucleic Acids Research*, 46(20):e120–e120, November 2018.
 - [6] Ben Langmead, Cole Trapnell, Mihai Pop, and Steven L. Salzberg. Ultra-fast and memory-efficient alignment of short DNA sequences to the human genome. *Genome Biology*, 10(3):R25, March 2009.
 - [7] Christopher Pockrandt, Mai Alzamel, Costas S. Iliopoulos, and Knut Reinert. GenMap: Fast and Exact Computation of Genome Mappability. *bioRxiv*, page 611160, April 2019.
 - [8] Parameswaran Ramachandran, Gareth A. Palidwor, Christopher J. Porter, and Theodore J. Perkins. MaSC: mappability-sensitive cross-correlation for estimating mean fragment length of single-end short-read sequencing data. *Bioinformatics*, 29(4):444–450, February 2013.
 - [9] Daniel R. Zerbino, Nathan Johnson, Thomas Juettemann, Steven P. Wilder, and Paul Flicek. WiggleTools: parallel processing of large collections of genome-wide datasets for visualization and statistical analysis. *Bioinformatics*, 30(7):1008–1009, April 2014.